

$$r_1 = \{k_0[\text{H}^+]^2[\text{BrO}_3^-] + k_c''[\text{H}^+]^2[\text{VO}_2^+][\text{BrO}_2]\}[\text{MB}] \quad (18)$$

But,

$$[\text{VO}_2^+][\text{BrO}_2] = K_{10}[\text{VO}_2^+][\text{BrO}_3^-] \quad (19)$$

where k_{10} is the equilibrium constant for eq 10. Substituting eq 19 into eq 18, we get

$$r_1 = \{k_0[\text{H}^+]^2[\text{BrO}_3^-] + k_c[\text{H}^+]^2[\text{VO}_2^+][\text{BrO}_3^-]\}[\text{MB}] \quad (20)$$

where $k_c = k_c'' = k_c''K_{10}$, the catalytic constant.

In the presence of excess concentrations of H^+ and bromate ions, eq 20 can be written as

$$r_1 = k_0' + k_c'[\text{VO}_2^+][\text{MB}] \quad (21)$$

and

$$r_1 = k_1'[\text{MB}] \quad (22)$$

where $k_c' = k_c[\text{H}^+]^2[\text{BrO}_3^-]$, the pseudo-first-order rate constant for catalyzed reaction.

$$k_1' = k_0' + k_c'[\text{VO}_2^+],$$

the overall pseudo-first-order rate coefficient (23)

The plot of k_1' versus $[\text{VO}_2^+]$ should yield a straight line with an intercept k_0' and a gradient of value k_c' ,²² which is observed to be the case (Table IV). For the later stages of the reaction with significant amount HOBr , the overall rate equation can be represented by eq 24, which explains the slow and fast phases of the reaction and also the role of bromide ion.

$$r_1 = k_0[\text{H}^+]^2[\text{BrO}_3^-] + k_8[\text{H}^+][\text{BrO}_3^-]^{1/3}[\text{Br}^-]^{2/3} + k_c[\text{H}^+]^2[\text{VO}_2^+][\text{BrO}_3^-][\text{MB}] \quad (24)$$

Acknowledgment. We thank the Dr. P. G. McDowell International Centre for Insect Physiology and Ecology, Nairobi, for running the mass spectra of the product samples and Deutscher Akademischer Austauschdienst, Federal Republic of Germany, for financial support.

Registry No. MB, 61-73-4; Azure A, 531-53-3; V(V), 22537-31-1.

Kinetics and Product Studies of the Reaction $\text{ClO} + \text{BrO}$ Using Discharge-Flow Mass Spectrometry

Randall R. Friedl* and Stanley P. Sander

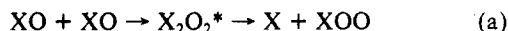
Jet Propulsion Laboratory, California Institute of Technology, Pasadena, California 91109

(Received: August 10, 1988; In Final Form: December 20, 1988)

The kinetics and product branching ratios of the $\text{BrO} + \text{ClO}$ reaction have been characterized at 1 Torr of total pressure over the temperature range 220–400 K with the technique of discharge-flow mass spectrometry. The measured overall reaction rate coefficient is $k_1 = (4.70 \pm 0.50) \times 10^{-12} \exp[(320 \pm 40)/T] \text{ cm}^3 \text{ molecule}^{-1} \text{ s}^{-1}$. Three product channels, identified as $\text{Br} + \text{ClOO}$ (1a), $\text{Br} + \text{OCIO}$ (1b), and $\text{BrCl} + \text{O}_2$ (1c) have been quantified: $k_{1a} = (2.9 \pm 1.0) \times 10^{-12} \exp[(217 \pm 50)/T] \text{ cm}^3 \text{ molecule}^{-1} \text{ s}^{-1}$; $k_{1b} = (1.6 \pm 0.4) \times 10^{-12} \exp[(426 \pm 50)/T] \text{ cm}^3 \text{ molecule}^{-1} \text{ s}^{-1}$; $k_{1c} = (5.8 \pm 2.0) \times 10^{-13} \exp[(168 \pm 50)/T] \text{ cm}^3 \text{ molecule}^{-1} \text{ s}^{-1}$. On the basis of these results, it is argued that the reaction mechanism for $\text{ClO} + \text{BrO}$, like those of halogen monoxide self-reactions, involves metastable intermediate formation. In addition, emphasis is placed on the significant impact of these results on current models of stratospheric ozone depletion, which neglect channel 1c and the temperature dependence of k_1 .

Introduction

The gas-phase self-reactions of halogen monoxide radicals (XO , $\text{X} = \text{F}, \text{Cl}, \text{Br}, \text{I}$) exhibit a range of product channels and pressure and temperature dependences.¹⁻⁶ The ClO self-reaction, for example, is strongly dependent on pressure and yields a host of chlorine-containing products, i.e., Cl , Cl_2 , OCIO , and Cl_2O_2 . The BrO self-reaction, on the other hand, displays no pressure dependence and apparently produces only Br and Br_2 as the bromine-containing species. The mechanisms for all of these reactions, however, are thought to be the same: formation of a metastable intermediate (X_2O_2^*) followed by collisional stabilization or unimolecular decomposition along one of several possible potential energy surfaces.



According to this mechanism, the relative importance of the possible product channels depends on the rates at which the isomeric forms of X_2O_2 (XOOX , XOXO , etc.) are produced, the stabilization rates and thermodynamic stabilities of the dimers, and the rates for X_2O_2^* decomposition. Experimental studies of the halogen oxide self-reactions have begun to provide, only recently, the information required to critically assess the validity of this mechanism as well as to provide it with a rigorous, quantitative foundation.

Cross-reactions of halogen monoxide radicals can provide additional insight into the details of halogen oxide reaction mechanisms and thermochemistry. The data base for these types of reactions, however, is limited to a few, contradictory reports on the reaction between ClO and BrO . Basco and Dogra,⁷ in the earliest of these studies, concluded that the reaction proceeds at 298 K with a rate coefficient of $(2.4 \pm 0.5) \times 10^{-12} \text{ cm}^3 \text{ molecule}^{-1} \text{ s}^{-1}$ and yields mainly BrCl and O_2 . Subsequently, Clyne and Watson⁸ measured a room-temperature rate coefficient of $(1.34 \pm 0.3) \times 10^{-11} \text{ cm}^3 \text{ molecule}^{-1} \text{ s}^{-1}$ and provided strong evidence for the equal importance of reaction channels yielding $\text{Br} + \text{ClOO}$ and $\text{Br} + \text{OCIO}$. Both of these studies were limited, however, by the fact that the $\text{ClO} + \text{BrO}$ reaction was studied as part of a complex reaction system in which a multitude of reactions were occurring.

(1) Sander, S. P. *J. Phys. Chem.* **1986**, *90*, 2194.

(2) Sander, S. P.; Watson, R. T. *J. Phys. Chem.* **1981**, *85*, 4000.

(3) Hayman, G. D.; Davies, J. M.; Cox, R. A. *Geophys. Res. Lett.* **1986**, *13*, 1347.

(4) Clyne, M. A. A.; McKenney, D. J.; Watson, R. T. *J. Chem. Soc., Faraday Trans. 1* **1975**, *71*, 322.

(5) Wagner, H. G.; Zetsch, C.; Warnatz, J. *Ber. Bunsen-Ges. Phys. Chem.* **1972**, *76*, 526.

(6) Clyne, M. A. A.; Watson, R. T. *J. Chem. Soc., Faraday Trans. 1* **1974**, *70*, 1109.

(7) Basco, N.; Dogra, S. K. *Proc. R. Soc. London, A* **1971**, *323*, 417.

(8) Clyne, M. A. A.; Watson, R. T. *J. Chem. Soc., Faraday Trans. 1* **1977**, *73*, 1169.

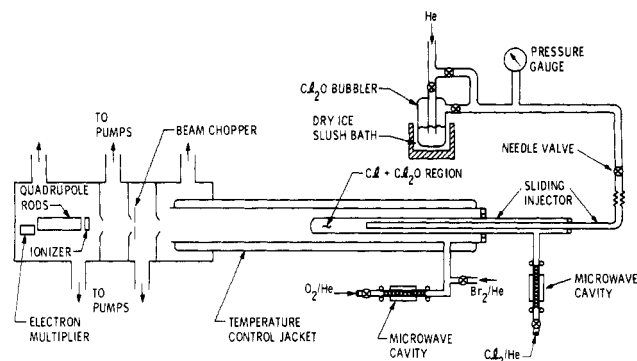
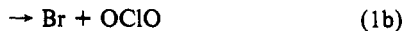
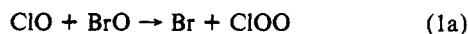


Figure 1. Schematic of the discharge-flow mass spectrometer apparatus. The source configuration shown was typical of most BrO decay measurements.

Recently, Hills et al.⁹ have studied this reaction in a more direct fashion under pseudo-first-order conditions in excess ClO. They report product yields similar to those obtained by Clyne and Watson. However, the reported overall reaction rate coefficient, $(8.2 \pm 1.0) \times 10^{-12} \text{ cm}^3 \text{ molecule}^{-1} \text{ s}^{-1}$ (no temperature dependence observed), is significantly lower than that of Clyne and Watson. In addition, they place an upper limit on the channel-producing BrCl, which is approximately an order of magnitude below the determination of Basco and Dogra.

Inadequacies in the current understanding of halogen oxide reactions have been particularly exposed by the recent discovery of dramatic ozone depletion in the Antarctic stratosphere.¹⁰ Theories for this phenomenon have been proposed, which incorporate poorly known characteristics of the ClO self-reaction and the reaction of ClO with BrO.^{11,12} The impact of the ClO + BrO reaction on Antarctic chemistry, in particular, depends critically on the branching ratios, at stratospheric temperatures (190–220 K), of the channels giving Cl, OClO, and BrCl, as well as on the absolute rate constant for the overall process.

In the present study, we have obtained kinetics data from 220–400 K for the following reaction channels of ClO + BrO:



Experimental results were obtained at a pressure of 1 Torr from a discharge-flow reactor coupled to a quadrupole mass spectrometer. The apparatus is similar to those employed by Hills et al.⁹ and Clyne and Watson.⁸ In the present study, however, we have employed a wider variety of chemical source conditions in order to fully elucidate the reaction pathways. We have also obtained kinetics data for reaction 1 at higher pressures using the flash photolysis-ultraviolet absorption technique. The results of that work are presented in the following paper in this issue.

Experimental Section

Investigations of the ClO + BrO reaction were conducted with an 80-cm-length, 2.54-cm-o.d. Pyrex tube that was coated with halocarbon wax (Figure 1). Temperature control (220–400 K) of the reactor was achieved by circulation of cooled methanol or

heated ethylene glycol through an outer Pyrex jacket. A gaseous flow, consisting predominantly of He and ranging from 10 to 25 (STP) $\text{cm}^3 \text{ s}^{-1}$, was established within the reactor by connection to a 50 cfm mechanical pump (Welch 1398). The resulting gaseous residence times in the reactor were between 20 and 50 ms. In order to protect the pump, chlorine- and bromine-containing gases were trapped at liquid nitrogen temperatures downstream of the reactor.

Mass spectrometric detection of reactants and products was employed with continuous sampling at the downstream end of the flow tube through a three-stage beam inlet system. The extranuclear spectrometer consisted of an electron-impact ionizer, operated at 25 eV, a quadrupole mass filter, and a channeltron. Ion beams were detected by lock-in analog signal processing. Beam modulation was accomplished with a 200-Hz tuning fork type chopper placed inside the second stage of the mass spectrometer.

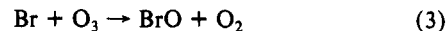
Halogen monoxide radicals were added into the reactor through a 120-cm-length, 0.63-cm-o.d. sliding Pyrex injector tube that was concentric with the reactor tube and a 20-cm-length, 1.2-cm-o.d. fixed side arm positioned at the upstream end of the reactor. Both chemical source regions were coated on the inside with halocarbon wax. The sliding injector was also coated with halocarbon wax on the outside surface. Residence times within the chemical source regions varied depending on the partitioning of the mass flow but were typically 100 ms in the sliding injector and 20 ms in the side arm. Contact times between the two radical flows were varied by movement of the injector.

Radical generation inside the source regions was accomplished by chemical titrations involving atomic and molecular precursors. Atomic species were generated from diatomic precursors such as Cl₂, Br₂, and O₂ in Evenson-type microwave cavities that were attached to both the injector and the side arm. BrO radicals were generated for most experimental runs by the reaction of oxygen atoms with excess molecular bromine:



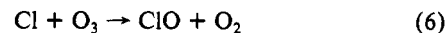
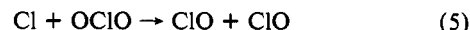
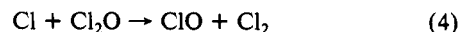
$$k_2(298 \text{ K}) = 1.4 \times 10^{-11} \text{ cm}^3 \text{ molecule}^{-1} \text{ s}^{-1}{}^{13}$$

For one set of experiments, BrO was generated by titration of bromine atoms with excess ozone:



$$k_3 = 1.7 \times 10^{-11} \exp(-800/T) \text{ cm}^3 \text{ molecule}^{-1} \text{ s}^{-1}{}^{14}$$

ClO radicals were generated by reaction of chlorine atoms with either dichlorine monoxide, chlorine dioxide, or ozone.



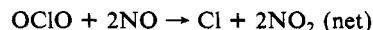
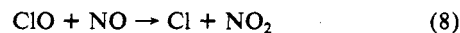
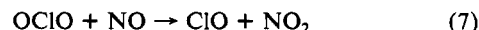
$$k_4 = 9.8 \times 10^{-11} \text{ cm}^3 \text{ molecule}^{-1} \text{ s}^{-1}{}^{14}$$

$$k_5 = 5.9 \times 10^{-11} \text{ cm}^3 \text{ molecule}^{-1} \text{ s}^{-1}{}^{14}$$

$$k_6 = 2.9 \times 10^{-11} \exp(-260/T) \text{ cm}^3 \text{ molecule}^{-1} \text{ s}^{-1}{}^{14}$$

For a particular set of experiments, the choice of ClO source and of source conditions (e.g., excess Cl) was predicated on considerations of mass spectral interferences as well as possible complications due to secondary chemistry.

Extraction of kinetics parameters from temporal profiles of reactants and products required absolute concentration calibrations of mass spectral signals. Calibrations for ClO ($m/e = 51$), BrO ($m/e = 95$), OClO ($m/e = 67$), and O₃ ($m/e = 48$) were accomplished by chemical conversion to NO₂ with excess NO. The stoichiometries of these titrations were 1 in all cases except for OClO where it was 2, i.e.



(9) (a) Hills, A. J.; Cicerone, R. J.; Calvert, J. G.; Birks, J. W. *J. Phys. Chem.* **1988**, *92*, 1853; (b) *Nature* **1987**, *328*, 405.

(10) Farman, J. C.; Gardiner, B. G.; Shanklin, J. D. *Nature* **1985**, *315*, 207.

(11) McElroy, M. B.; Salawitch, R. J.; Wofsy, S. C.; Logan, J. A. *Nature* **1986**, *321*, 759.

(12) Molina, L. T.; Molina, M. J. *J. Phys. Chem.* **1987**, *91*, 433.

(13) Baulch, D. L.; Cox, R. A.; Hampson, R. F.; Kerr, J. A.; Troe, J.; Watson, R. T. *J. Phys. Chem. Ref. Data* **1984**, *13*, 1259.

(14) Demore, W. B.; Molina, M. J.; Sander, S. P.; Golden, D. M.; Hampson, R. F.; Kurylo, M. J.; Howard, C. J.; Ravishankara, A. R. *Chemical Kinetics and Photochemical Data for Use in Stratospheric Modeling*; JPL Publication 87-41; Jet Propulsion Laboratory: Pasadena, CA, 1987.

The resultant NO₂ signals observed at $m/e = 46$ were converted to concentrations by comparison with previously obtained NO₂ calibrations. NO₂ signals, as well as those from Br₂ ($m/e = 160$), BrCl ($m/e = 116$), and O₂ ($m/e = 32$), were calibrated by comparison with measured flows of those species. Detection limits for the molecules and radicals of interest were found to range between 1×10^8 and 5×10^8 molecules cm⁻³. One molecule of interest, ClOO, could not be detected mass spectrometrically due to its rapid decomposition under the experimental conditions.¹⁴

The gases used in these experiments were obtained from Matheson and Alphagaz with the following purities: He, 99.999%; NO, 99% (further purified by passage through an Ascarite trap); NO₂, 99.5%; Cl₂, 99.99%; O₂, 99.99%. Isotopically labeled oxygen, ³⁶O₂, used in one set of experiments, was obtained with 98% purity from Cambridge Isotopes. Br₂ was obtained from Fisher (99.5%) and was purified by vacuum distillation at 196 K. A gaseous sample of Br₂ was drawn off the liquid, diluted with He, and stored in a glass reservoir. BrCl was prepared by mixing an excess of Cl₂ (20–100 Torr) with Br₂ (2–6 Torr). An equilibrium mixture of BrCl, Br₂, and Cl₂, greatly favoring BrCl relative to Br₂, was allowed to develop over a 24-h period. The partial pressure of BrCl in the mixture was determined with the equilibrium constant¹⁵

$$K_{\text{eq}} = 7.63 = [\text{BrCl}]^2 / ([\text{Br}_2][\text{Cl}_2])$$

The molecular precursors of ClO were obtained as follows. Cl₂O was prepared by reaction of Cl₂ with yellow HgO (Baker) at 196 K.¹⁶ The reaction mixture was allowed to stand for several days, whereupon the Cl₂O was collected in a trap held at 97 K as the product of a room-temperature vacuum distillation. The collected Cl₂O was purified by vacuum distillation at 155 K (ethanol bath) and subsequently stored at 97 K. During experimental runs, Cl₂O was maintained at 196 K and was bubbled into the reactor with a measured flow of He. O₃ was produced in an ac discharge (Welsbach Model T-408) of O₂ and stored on silica gel at 196 K. O₃ was eluted into the reactor in a manner similar to that of Cl₂O. To dispose of the O₃ safely after passage through the reaction chamber, a 50-cm-long quartz tube wrapped with nichrome wire was placed upstream of the liquid nitrogen trap and the mechanical pump. With the quartz tube heated to 900 K, nearly all of the O₃ decomposed within that region. Only small amounts of O₃ were collected in the liquid N₂ trap after hours of experimentation. OCIO was directly added into the reactor after it was generated by flowing Cl₂/He mixtures through a column packed with NaClO₂ (Baker). The Cl₂ flow rates were sufficiently low to insure nearly complete removal of the Cl₂ before entry into the reactor.

Results

Kinetics of BrO Decays. The behavior of BrO [(1–3) × 10¹¹ molecules cm⁻³] was investigated in the presence of excess ClO [(1–20) × 10¹² molecules cm⁻³]. For this set of experiments, BrO was produced by titration of oxygen atoms with excess molecular bromine [(5–20) × 10¹³ molecules cm⁻³] (reaction 2). The advantages of this BrO source over one involving excess O₃ (reaction 3) were 2-fold. First, possible regeneration of BrO within the reactor by reaction of O₃ with any bromine atoms produced from reactions 1a or 1b was avoided. Second, the excess Br₂ acted as a scavenger of chlorine atoms.



$$k_9 = 1.7 \times 10^{-10} \text{ cm}^3 \text{ molecule}^{-1} \text{ s}^{-1} \quad (17)$$

Chlorine atoms, produced in reaction 1a and in the ClO self-reaction, if left unscavenged, were capable of depleting BrO by the reaction



$$k_{10} = 2.0 \times 10^{-10} \text{ cm}^3 \text{ molecule}^{-1} \text{ s}^{-1} \quad (18)$$

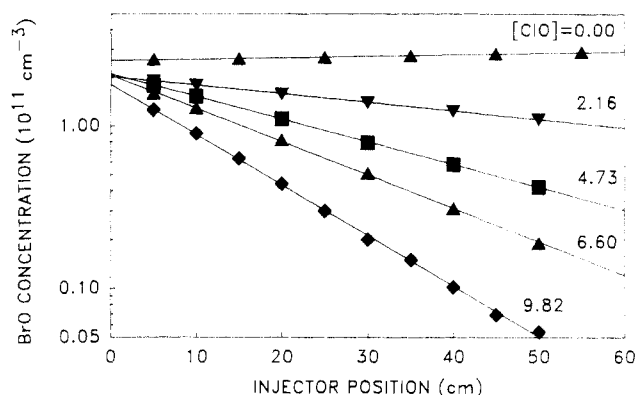
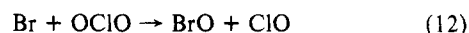
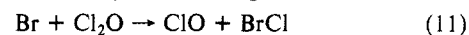


Figure 2. BrO decay in the presence of ClO at 245 K. Numbers are ClO concentrations (10¹² molecule cm⁻³). For [ClO] = 0.0, the increase in BrO signal is due to the decrease of BrO loss on the injector.

ClO was generated for these experiments by titration of Cl₂O or OCIO with excess Cl. The use of excess Cl atoms alleviated difficulties due to reactions of the molecular precursors with bromine atoms generated by the O + Br₂ reaction



$$k_{11} = 3.8 \times 10^{-12} \text{ cm}^3 \text{ molecule}^{-1} \text{ s}^{-1} \quad (14)$$

$$k_{12} = 4.2 \times 10^{-13} \text{ cm}^3 \text{ molecule}^{-1} \text{ s}^{-1} \quad (15)$$

In addition, the removal of Cl₂O and OCIO simplified the interpretation of the mass spectral signals observed at $m/e = 51$.

At 298 K, kinetics data were obtained with the BrO admitted into the reactor through the 1.2-cm-o.d. side arm as well as through the 0.63-cm-o.d. sliding injector. Reversal of the ClO and BrO sources was attempted in order to investigate possible effects on source chemistry due to the higher pressures, increased surface to volume ratio, and longer reaction times associated with the sliding injector. At temperatures other than 298 K, however, the sliding injector could not be used for BrO generation. This was due to the significant temperature dependence of BrO loss inside the injector. As the injector was moved, the fraction of injector surface held at ambient temperature relative to the surface that was cooled or heated varied. This variation resulted in relatively large and irreproducible fluctuations in the BrO concentrations admitted to the reactor. This effect was much less pronounced for ClO. Accordingly, for temperatures other than 298 K, BrO was added to the reactor through the fixed side arm and ClO was added through the sliding injector.

First-order BrO decay rates, k_1' , were obtained from the slopes of plots of logarithm of BrO signal vs injector distance (Figure 2) and the measured flow velocity. The observed decays were corrected for axial diffusion and for loss of BrO on the injector according to eq I,¹⁸ where D is the diffusion coefficient, \bar{v} is the

$$k_1^{\dagger} = k_1' (1 + k_1' D / \bar{v}^2) + k_p \quad (I)$$

mean bulk flow velocity, and k_p is the first-order loss of BrO on the outside surface of the sliding injector. For experiments at 298 K where BrO was added through the sliding injector, eq I was modified by substitution of the term $-k_w$ (first-order BrO loss on the reactor wall) for k_p . The diffusion coefficient for BrO in He was estimated from the data of Marrero and Mason¹⁹ for krypton in helium. The estimated values of D ranged from 0.39 atm cm² s⁻¹ at 220 K to 1.07 atm cm² s⁻¹ at 400 K. Corrections for axial diffusion, in parentheses in eq I, were always less than 2%. Losses of BrO on the injector and reactor walls were measured before every set of experiments and were always less than 5 s⁻¹.

The bimolecular rate constants, k_1 , for the overall decays of BrO at various temperatures were determined from the slopes of least-square fits to the plots of k_1^{\dagger} vs ClO concentrations (Figure

(15) Loewenstein, L. M.; Anderson, J. G. *J. Phys. Chem.* **1984**, *88*, 6277.
 (16) Schack, C. J.; Lindahl, C. B. *Inorg. Nucl. Chem. Lett.* **1967**, *3*, 387.
 (17) Toohy, D. W.; Anderson, J. G. *J. Phys. Chem.* **1988**, *92*, 1705.

(18) Howard, C. J. *J. Phys. Chem.* **1979**, *83*, 3.

(19) Marrero, T. R.; Mason, E. A. *J. Phys. Chem. Ref. Data* **1972**, *1*, 3.

TABLE I: Summary of ClO + BrO Rate Coefficient and Product Yield Data^a

ref	temp, K	k_1 , 10^{-11} cm ³ molecule ⁻¹ s ⁻¹	k_{1a}/k_1	k_{1b}/k_1	k_{1c}/k_1	k_{1a+1c}/k_1
7	298	0.24			1.0 (assumed)	
8	298	1.34	0.5	0.5		
17	298	1.4		0.45		
9	241	0.80	0.42	0.50		
	305	0.84	0.44	0.53	<0.02	
	408	0.83				
this work ^b	220	2.15 ± 0.30 (27)		0.55 ± 0.07 (18)	0.06 ± 0.03 (28)	0.45 ± 0.10 (33)
	245	1.72 ± 0.22 (11)				
	268	1.54 ± 0.20 (12)				
	298	1.29 ± 0.19 (40)		0.48 ± 0.07 (21)	0.08 ± 0.03 (13)	0.48 ± 0.10 (54)
	350	1.21 ± 0.20 (7)				
	400	1.10 ± 0.20 (12)		0.44 ± 0.07 (12)	0.08 ± 0.03 (18)	0.52 ± 0.12 (33)

^aRate expressions inferred from the present work: $k_{1a} = (2.9 \pm 1.0) \times 10^{-12} \exp[(217 \pm 50)/T]$ cm³ molecule⁻¹ s⁻¹, $k_{1b} = (1.6 \pm 0.4) \times 10^{-12} \exp[(426 \pm 50)/T]$ cm³ molecule⁻¹ s⁻¹, and $k_{1c} = (5.8 \pm 2.0) \times 10^{-13} \exp[(168 \pm 50)/T]$ cm³ molecule⁻¹ s⁻¹. ^bNote: Numbers of experimental measurements are given in parentheses.

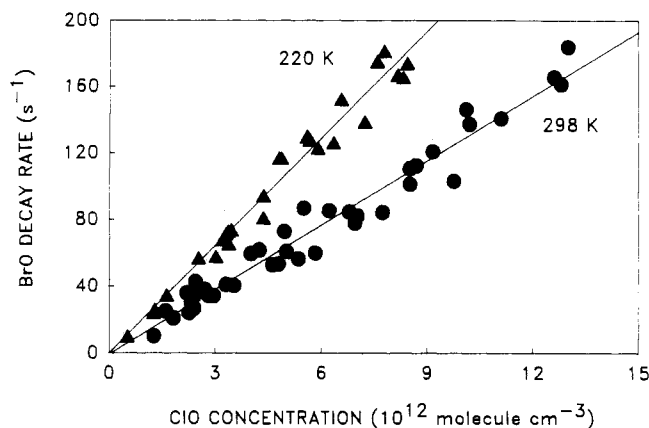


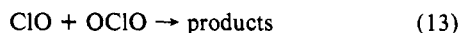
Figure 3. First-order decay rates, k^1 , of BrO as a function of [ClO] at 298 K (●) and 220 K (▲).

3). The set of experimentally determined rate coefficients are shown in Table I and Figure 4. The data can be fit to an Arrhenius expression of the form

$$k_1 = (4.70 \pm 0.50) \times 10^{-12} \exp[(320 \pm 40)/T] \text{ cm}^3 \text{ molecule}^{-1} \text{ s}^{-1}$$

where the quoted uncertainty is at the 95% confidence limit.

Product Yields of OCIO. The experimental conditions employed for the determinations of BrO decays, i.e., Br₂ in excess over oxygen atoms and chlorine atoms in slight excess over Cl₂O, were also well suited to observations of OCIO production. The presence of excess Br₂ resulted in rapid removal of chlorine atoms (reaction 9) on a short time scale compared to the formation of OCIO by reaction 1b. Consequently, OCIO removal by chlorine atoms (reaction 5) was negligible. Bromine atom concentrations, resulting from reactions 2 and 9, were significant. However, the removal rate of OCIO by Br (reaction 12) was on the order of 1 s⁻¹, assuming an upper limit of 5 × 10¹² molecules cm⁻³ for Br concentrations, and could be neglected. The possibility of OCIO removal by ClO



was investigated in a separate experiment that utilized the titration of Cl with excess Cl₂O as the ClO source. The observed temporal behavior of OCIO in this system provided no evidence for the occurrence of reaction 13 ($k_{13} \leq 1 \times 10^{-13}$ cm³ molecule⁻¹ s⁻¹).

Production of OCIO by reaction 1b was quantified relative to loss of BrO. This was accomplished by monitoring changes in BrO and OCIO concentrations when the ClO source (i.e., chlorine atom discharge) was turned on and off. Small amounts of signal at $m/e = 67$ were also generated by the ClO self-reaction. This background level was taken into account by turning the BrO source (i.e., oxygen atom discharge) off. Data were obtained for a variety of reaction times and reactant concentrations (Figure 5). The observed OCIO yields (k_{1b}/k_1) were 0.55 ± 0.07 at 220 K, 0.46

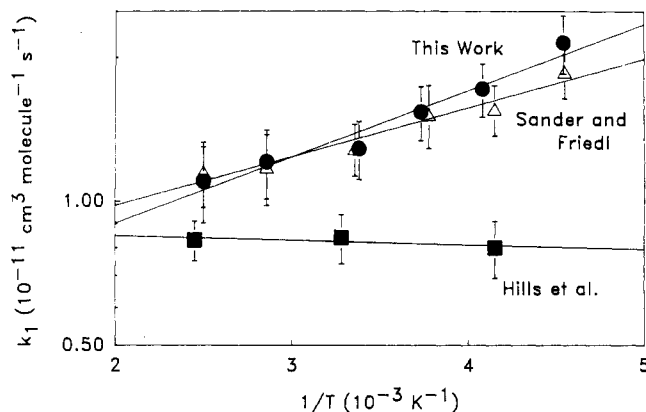


Figure 4. Temperature dependence of k_1 as observed in this study (●), by Hills et al.⁹ (■), and by Sander and Friedl (Δ) from work reported in the following article in this issue.

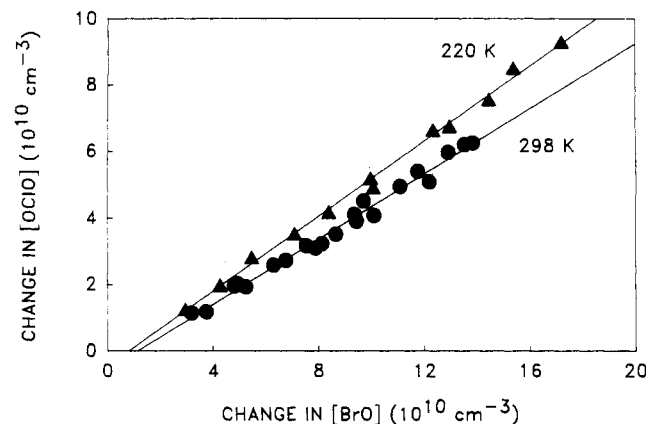
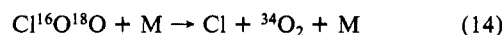
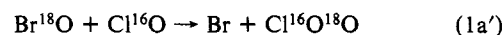
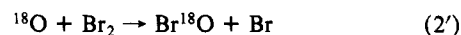


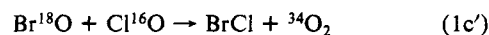
Figure 5. Production of OCIO as a function of BrO loss at 298 K (●) and 220 K (▲).

± 0.07 at 298 K, and 0.44 ± 0.07 at 400 K. With BrO added through the sliding injector, the OCIO yield was 0.49 ± 0.07 at 298 K (Table I).

Product Yields of O₂. Substitution of isotopically labeled oxygen, ³⁶O₂, as the oxygen atom precursor in the microwave discharge allowed for monitoring of molecular oxygen production from reaction 1.



$$k_{14} = 8.7 \times 10^{-9} (T/300)^{-1.4} \exp(-3000/T) \text{ cm}^3 \text{ molecule}^{-1} \text{ s}^{-1} \quad (14)$$

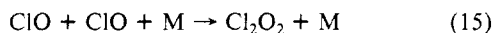


Data for Br¹⁸O and ³⁴O₂ were obtained and analyzed in a manner similar to that employed for OCIO measurements. Calibration factors for ³⁴O₂ ($m/e = 34$) and Br¹⁸O ($m/e = 99$) were assumed to equal those determined for the more abundant isotopes. These assumptions were checked indirectly as follows. First, calibration factors for ³²O₂ and ³⁶O₂ were measured and found to be equal within experimental error. Second, a relative calibration factor was determined for Br¹⁸O by titration with N¹⁶O and detection of N³⁴O₂. The signal ratio between Br¹⁸O and N³⁴O₂ was found to be similar to the ratio obtained between Br¹⁶O and N³²O₂. A reasonable, although not unique, interpretation of the above results is that the mass spectral calibrations are insensitive to the isotopic identities of O₂, NO₂, and BrO.

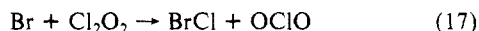
O₂ production was investigated at 220 and 298 K. A significant amount of ³⁴O₂ was produced in the BrO source region due, perhaps, to recombination of isotopically different oxygen atoms and to self-reaction of BrO isotopes. This background signal was readily accounted for by turning off the ClO source. The molecular oxygen yields from reaction 1 ($[k_{1a} + k_{1c}]/k_1$) were found to be 0.45 ± 0.10 at 220 K, 0.47 ± 0.10 at 298 K, and 0.54 ± 0.10 at 298 K with BrO added through the sliding injector.

Product Yields of BrCl in Excess Br₂. The presence of a high Br₂ concentration ($\geq 1 \times 10^{13}$ molecules cm⁻³) in the reactor ensured rapid and complete conversion of chlorine atoms to BrCl through reaction 9. Consequently, the combined yield of BrCl from channels 1a and 1c could be determined in a reaction system containing excess Br₂. In order to accomplish these measurements, a ClO source was required that did not contain excess Cl or Cl₂O due to the substantial interference to the BrCl signal caused by the reaction of these excess reagents with Br₂ or Br (reactions 9 and 11). The ClO source chosen for this set of experiments, therefore, consisted of Cl and a slight excess of OCIO. Reaction of the excess OCIO with Br (reaction 12) did not directly interfere with BrCl measurements and had only a slight impact on BrO concentrations under the experimental conditions employed. The BrO source for these experiments was the same as used for the previously described measurements, i.e., O + Br₂.

As with the other product yield studies, production of BrCl was quantified relative to the loss of BrO. A background source of BrCl due to Cl atoms generated in the ClO self-reaction was quantified by turning off the oxygen atom discharge while maintaining the molecular bromine flow. With BrO added through the sliding injector at 298 K, the measured BrCl yield in excess Br₂ ($[k_{1a} + k_{1c}]/k_1$) was 0.46 ± 0.07 . This value compares quite favorably with the value obtained from the O₂ yield experiment. However, when BrO was added through the side arm, BrCl yields approaching unity were measured. We believe that these large values were due to interference from reactions of bromine atoms with the ClO dimer, Cl₂O₂.



$$k_{15} = 4.0 \times 10^{-32} (T/300)^{-2} \text{ cm}^6 \text{ molecule}^{-2} \text{ s}^{-1} \quad (\text{M} = \text{N}_2)^{14}$$



Unlike the previous sets of experiments, significant dimer concentrations in the source region were possible in this experiment due to the removal of chlorine atoms by the excess OCIO. Chlorine atoms are known to react rapidly with the ClO dimer and would otherwise ensure its complete removal.³

As a check of the ClO dimer hypothesis, the mass spectrometer was set at $m/e = 102, 104,$ and 106 . With the BrO source off, a signal was detected at all of these settings in ratios consistent with that expected for Cl₂O₂. We were unable, however, to calibrate these signals due to the lack of a simple chemical titration scheme. Therefore, as a further check of this hypothesis, the 0.63-cm-o.d. injector was replaced with one 0.95 cm in outer diameter. The total pressure inside the larger injector was found to be nearly 3 times less than in the smaller one. Consequently, the pressure-dependent formation of Cl₂O₂ was significantly suppressed in the 0.95-cm-o.d. tube. BrCl yields measured with

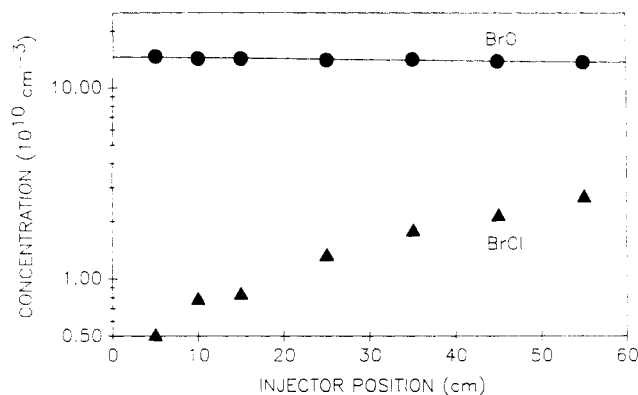


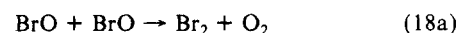
Figure 6. Concentration profiles of BrO (●) and BrCl (▲) in the presence of ClO (7×10^{12} molecules cm⁻³) and excess O₃ (4×10^{13} molecules cm⁻³) at 298 K. A least-squares fit (solid line) to the BrO data reveals a first-order reaction rate loss of 7 s^{-1} . The flow velocity in this experiment was 2280 cm s^{-1} , and the BrO loss on the injector was 3 s^{-1} .

this injector were 0.63 ± 0.10 at 220 K, 0.58 ± 0.10 at 298 K, and 0.66 ± 0.10 at 400 K. These results strongly implicate Cl₂O₂ in the secondary chemistry that produces BrCl. We consider the yields observed in these latter experiments to be upper limits to the true yields since Cl₂O₂ formation was not completely suppressed in the 0.95-cm-o.d. injector. The BrCl yield measured when ClO was made in the fixed side arm should be substantially free of this interference and should be considered the best method for measuring this quantity.

Product Yields of BrCl and OCIO in Excess O₃. Production of BrCl and OCIO from reaction 1 was also investigated in the presence of large concentrations of O₃ [$(1-5) \times 10^{14}$ molecules cm⁻³]. The addition of O₃ to the reactor was designed to prevent conversion of Cl, produced from reaction 1a, to BrCl by reaction with Br₂. Competition for the chlorine atoms, however, favors Br₂ relative to O₃ due to an order of magnitude difference in the rate constants for the respective reactions. In order to effectively inhibit reaction of Cl with Br₂ concentrations of O₃ over 1000 times greater than those of Br₂ were required. This condition could be achieved by employing as a BrO source the titration of Br with excess O₃. The advantage of this source was the use of low Br₂ concentrations compared to the titration of O with Br₂. The minimum amount of Br₂ admitted to the reactor from this source was determined by the efficiency of the microwave discharge for conversion of Br₂ to Br. This efficiency approached 90% for Br₂ concentrations near 2×10^{11} molecules cm⁻³ and He flow rates of $5 \text{ STP cm}^3 \text{ s}^{-1}$ through the discharge. Consequently, the amount of Br₂ admitted to the reactor after BrO generation was typically measured to be 2×10^{10} molecules cm⁻³. Meanwhile, concentrations of O₃ up to 5×10^{14} molecules cm⁻³ could be added to the reactor. The limit on the amount of O₃ added to the reactor was set by the maximum allowable He flow rate (half the total reactor flow) through the silica/O₃ trap and by the fraction of O₃ (1-5%) contained in the He flow.

Maintenance of large concentrations of O₃ and large $[\text{O}_3]/[\text{Br}_2]$ ratios ensured that Br and Cl were preferentially converted to BrO and ClO, respectively. As a consequence, the occurrence of reaction 1a or 1b was not allowed to result in decay of BrO or formation of BrCl. Nevertheless, both decay of BrO and formation of BrCl were observed in this system (Figure 6). We attribute these observations to the existence of reaction 1c.

The rate coefficient for reaction 1c was estimated from BrO decay data to be $1 \times 10^{-12} \text{ cm}^3 \text{ molecule}^{-1} \text{ s}^{-1}$ at all experimental temperatures (220, 298, and 400 K). The contribution to the observed BrO decay from the reaction



$$k_{18a} = 6 \times 10^{-14} \exp(600/T) \text{ cm}^3 \text{ molecule}^{-1} \text{ s}^{-1}{}^{14}$$

was on the order of 0.2 s^{-1} and hence could be neglected. This analysis was necessarily approximate, however, since the measured BrO decays never exceeded 20 s^{-1} even at the highest ClO con-

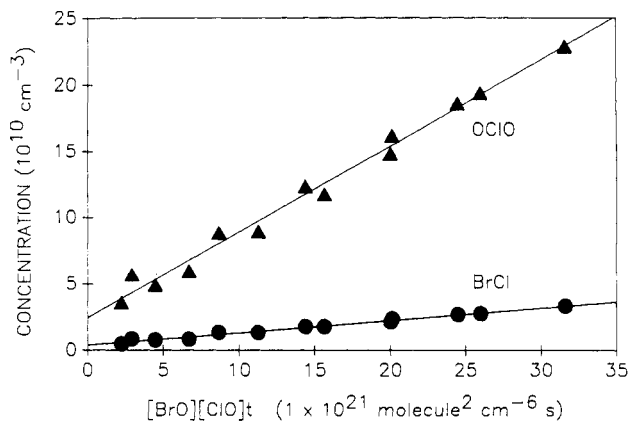


Figure 7. BrCl (●) and OCIO (▲) concentrations plotted as functions of the product of reaction time and BrO and ClO concentrations. Experiments were conducted at 298 K in excess O₃.

centrations. In addition, the initial decay rates (i.e., at short reaction times) were larger than at later times on account of the finite time required for re-formation of BrO by reaction 3. This effect was more apparent at 220 K due to the decrease in the rate coefficient for reaction 3.

Due to the rapid regeneration of BrO in these experiments, production of BrCl or OCIO could not be quantified relative to BrO loss. Instead, rate coefficients for reactions 1b and 1c were determined directly from the rates of OCIO and BrCl production and a knowledge of the reaction time and the BrO and ClO concentrations. In the case of BrCl, the production rate is given by

$$d[\text{BrCl}]/dt = k_{1c}[\text{ClO}][\text{BrO}] \quad (\text{II})$$

ClO concentrations, being in large excess over [BrO], were not observed to vary significantly during experimental runs; i.e., [ClO] = [ClO]₀. The BrO temporal behavior, on the other hand, is described by

$$[\text{BrO}] = [\text{BrO}]_0 \exp(-k_{1c}[\text{ClO}]_0 t) \quad (\text{III})$$

The solution to the differential equation is given by

$$[\text{BrCl}] = [\text{BrO}]_0 (1 - \exp(-k_{1c}[\text{ClO}]_0 t)) \quad (\text{IV})$$

When $k_{1c}[\text{ClO}]_0 t$ is small, as was the case in this experiment, the solution for [BrCl] becomes

$$[\text{BrCl}] = k_{1c}[\text{ClO}]_0 [\text{BrO}]_0 t \quad (\text{V})$$

BrCl data were analyzed according to eq V (Figure 7). An analogous equation was used to analyze the OCIO data. Small amounts of BrCl and OCIO, which were observed in this chemical system with the Br₂ discharge off, were subtracted from the signals obtained with the discharge on. Rate coefficients derived for channel 1c are (cm³ molecule⁻¹ s⁻¹) (1.2 ± 0.4) × 10⁻¹² at 220 K, (1.0 ± 0.4) × 10⁻¹² at 298 K, and (0.9 ± 0.3) × 10⁻¹² at 400 K. Rate coefficients derived for channel 1b are (8.0 ± 3.0) × 10⁻¹² at 200 K, (6.2 ± 2.0) × 10⁻¹² at 298 K, and (4.4 ± 1.5) × 10⁻¹² at 400 K.

OCIO product yields obtained from the O + Br₂ system compare favorably with the rate coefficients obtained in the O₃ experiment at both 298 and 400 K. At 220 K, however, the rate of OCIO production is comparatively less in the O₃ experiment. A puzzling feature of the excess O₃ experiment at 220 K was the presence of a relatively large background signal (one-fourth the total signal) at *m/e* = 67 when the Br₂ discharge was off. The presence of this signal was not easily rationalized and suggests that our determination of the OCIO production rate at 220 K in the presence of excess O₃ may have been affected by some as yet unidentified chemical process.

Discussion

The reactant decay and product yield data obtained in the present study can be combined to give the following Arrhenius

rate expressions for the three observed BrO + ClO reaction channels:

$$k_{1a} = (2.9 \pm 1.0) \times 10^{-12} \exp[(217 \pm 50)/T] \text{ cm}^3 \text{ molecule}^{-1} \text{ s}^{-1}$$

$$k_{1b} = (1.6 \pm 0.4) \times 10^{-12} \exp[(426 \pm 50)/T] \text{ cm}^3 \text{ molecule}^{-1} \text{ s}^{-1}$$

$$k_{1c} = (5.8 \pm 2.0) \times 10^{-13} \exp[(168 \pm 50)/T] \text{ cm}^3 \text{ molecule}^{-1} \text{ s}^{-1}$$

Like the total rate coefficient for reaction 1, each product channel is inversely dependent on temperature. The inverse temperature dependence or "negative activation energy" observed for k_{1a} supports the identification of ClOO + Br, not Cl + Br + O₂, as the nascent product set for this channel. Direct production of Cl, a process approximately 2 kcal mol⁻¹ endothermic, would be manifest in k_{1a} as a significant positive temperature dependence.

Negative activation energies have now been observed in a variety of bimolecular radical-radical reactions, including the BrO and IO self-reactions.¹⁴ Attempts to rationalize this behavior have focused on both "direct" and "complex" reaction mechanisms.²⁰⁻²² In the direct mechanism, the potential energy surface along the reaction coordinate has a single maximum and no minimum. An inverse temperature dependence can arise in this situation if the potential barrier is sufficiently small, i.e., a centrifugal barrier only, to allow the reaction to be dominated by attractive, long-range intermolecular forces.²⁰ Under these conditions it is possible for rotational state specific rate constants, $k_f(T)$, to increase with increasing translational temperature but decrease with increasing rotational level. When the rotational level dependence is stronger than the temperature dependence, the Maxwell-Boltzmann averaged rate constant will display inverse temperature behavior.

In the complex mechanism, the potential surface possesses a minimum corresponding to the formation of a chemically bonded intermediate. For this case, the inverse temperature dependence arises from the competition between product formation and reactant re-formation during dissociation of the chemical intermediate.^{21,22} As the temperature is lowered, this competition will increasingly favor product formation if the potential barrier for this process is lower than the initial energy of the reactants.

A special case of the complex mechanism occurs when the barrier to product formation is significantly lower than the initial reactant energy. Under this condition, dissociation of the intermediate back to reactants is not competitive, at any temperature, with dissociation to products. Accordingly, the rate limitation only involves formation of the intermediate. The relationship between the rate coefficient and temperature for this case will depend primarily on details of the potential surface in the reaction entrance channel. As in the direct mechanism, an inverse temperature dependence will have its origin in attractive, long-range intermolecular forces. This kinetic behavior is analogous to high-pressure limited behavior observed in termolecular reactions.

The XO self-reactions have typically been interpreted in terms of a complex mechanism.^{1,2,23} Evidence to support this interpretation, aside from observations of negative temperature dependences, include spectroscopic confirmation of Cl₂O₂ production in the ClO self-reaction^{12,24} and observations of pressure-dependent rate behavior in the ClO³ and IO¹ self-reactions where the pressure dependence is presumed to indicate stabilization of the reaction intermediate.

By analogy, one expects a similar mechanism for the XO cross-reactions. For the BrO + ClO reaction, two isomeric intermediate species can be rationalized. A species with the structure BrOOCl presumably decomposes to give ClOO and Br or BrCl

(20) Clary, D. C. *Mol. Phys.* **1984**, *53*, 3.

(21) Howard, M. J.; Smith, I. W. M. *Prog. React. Kinet.* **1983**, *12*, 55.

(22) Mozurkewich, M.; Benson, S. W. *J. Phys. Chem.* **1984**, *88*, 6429.

(23) Davies, J. M.; Hayman, G. D.; Cox, R. A. Presented at the 17th Informal Conference on Photochemistry, Boulder, CO, June 1986.

(24) Cox, R. A.; Hayman, G. D. *Nature* **1988**, *332*, 796.

TABLE II: Rate Parameters for the Bimolecular Components of Halogen Monoxide Self- and Cross-Reactions

reaction	A factor, ^a $10^{-12} \text{ cm}^3 \text{ molecule}^{-1} \text{ s}^{-1}$	E/R , ^a K	product yield	ref
ClO + ClO → products	1.60	+1250		14
→ 2Cl + O ₂			≈0.45	
→ Cl + OClO			≈0.10	
→ Cl ₂ + O ₂			≈0.45	
BrO + BrO → products	1.64	-225		2
→ 2Br + O ₂			0.84	
→ Br ₂ + O ₂			0.16	
IO + IO → products	3.46	-1020		1
→ 2I + O ₂			>0.95	
→ I ₂ + O ₂			<0.05	
ClO + BrO → products	4.70	-320		this work
→ Br + Cl + O ₂			0.42	
→ Br + OClO			0.50	
→ BrCl + O ₂			0.08	

^a Rate coefficient is defined here as $-d[\text{XO}]/dt = k[\text{XO}][\text{XO}] = [A \exp(-E/RT)][\text{XO}][\text{XO}]$.

and O₂, the latter set of products arising from a four-centered elimination. Formation of OClO and Br presumably follows from decomposition of the species BrOClO. As a test of this hypothesis, we attempted, but failed, to detect a mass spectral signal at $m/e = 146$ corresponding to either BrClO₂ isomer. Consequently, no direct evidence in support of a complex mechanism was obtained in the present study (the possibility of a pressure effect is investigated in the following article in this issue). The lack of signal at $m/e = 146$ certainly does not preclude a complex mechanism for reaction 1 but does imply that both BrClO₂ isomers are either weakly bound (<15 kcal mol⁻¹) or strongly fragmented upon electron impact at 25 eV.

Our identification of BrCl as a significant product of reaction 1 does, however, suggest a strong mechanistic similarity between the halogen monoxide cross- and self-reactions. Molecular halogen production has been suggested in both the BrO and ClO self-reactions in order to explain kinetics observations.^{2,23} In addition, emissions from electronically excited Cl₂ and Br₂ have been observed in chemical systems containing ClO and BrO, respectively.^{25,26} The prevalence of molecular halogen production in the XO reactions seemingly requires the presence of metastable intermediates to facilitate the complex intramolecular rearrangements.

Although a complex mechanism appears generally applicable to both the XO self- and cross-reactions, the wide range in rate coefficients and pressure and temperature dependences displayed by them (see Table II) suggests that important differences exist in the various complex potential surfaces. If one assumes that the barriers to intermediate formation are uniformly small for the XO + X'O reactions, as might be expected for interactions between two open-shell molecules, then the diversity in measured rate coefficients must be attributable to differences in the magnitudes of the barriers to product formation. For the ClO self-reaction, all of the product barriers appear to be larger than the initial energy of the reactants as indicated by the significant positive temperature dependence and small rate coefficient for the overall reaction. This conclusion is expected for the 2Cl + O₂ and Cl + OClO product channels because they are 2.6 and 3.1 kcal mol⁻¹ endothermic, respectively. The lack of a significant negative temperature dependence for the Cl₂ + O₂ product channel²³ suggests that the four-centered transition state associated with this path is at a substantially higher potential energy than the one associated with BrCl formation in the BrO + ClO reaction. This difference may be related to a near coincidence of the Br to Cl distance in BrOCl with that of the classical turning point of the $v = 7$ state of BrCl(³π_g).¹⁷

In contrast to the ClO self-reaction, the product barriers for the BrO + BrO, IO + IO, and BrO + ClO reactions are apparently less than the initial reactant energies as evidenced by the large rate coefficients and negative temperature dependences

measured for these reactions. For the IO self-reaction, Sander¹ has observed a pressure dependence in the relative product yields but not in the overall rate coefficient. On the basis of these observations, he concludes that formation of the intermediate is rate limiting, i.e., the special case of the complex mechanism is applicable, and that stabilization of the intermediate is competitive, at higher pressures, with the iodine atom forming channel. To the extent that these conclusions are valid, the similar magnitudes of the rate coefficients for BrO + ClO, BrO + BrO, and IO + IO can be interpreted as evidence that all of these reactions are predominantly rate limited by intermediate formation. The temperature dependences observed for reactions 1a and 1c in the present study also support the above conclusion. Presumably, both reaction channels proceed via a common intermediate (i.e., BrOCl). The product barrier for reaction 1c, however, should be significantly larger than the barrier for 1a. The absence of a large difference in the measured activation energies for these channels indicates, therefore, that their product barriers are not rate limiting.

Comparison to Previous Work. Values for the overall rate coefficient of reaction 1 at room temperature have been reported from four previous studies. The earliest of these, by Basco and Dogra,⁷ utilized flash photolysis of mixtures of Br₂ and OClO. As first pointed out by Clyne and Watson,⁸ Basco and Dogra did not measure the total reaction rate since the occurrence of reaction 1b did not result in removal of BrO or ClO in the flash experiment. Clyne and Watson also demonstrated that computational simplifications made by Basco and Dogra regarding the depletion of OClO and the constancy of the [ClO] to [BrO] ratio resulted in an underestimate of $k_{1a} + k_{1c}$. In the following article in this issue, we present a new flash photolysis study of reaction 1 that overcomes the deficiencies inherent in the Basco and Dogra study. The results of that study, shown in Figure 4, are in excellent agreement with the present work.

All other room-temperature values for k_1 were obtained at low pressure with the discharge-flow technique. Values of k_1 obtained by Clyne and Watson and Toohey et al.¹⁷ are in excellent agreement with the result of the present work, despite substantial differences in the chemical sources and detection techniques that were employed. Clyne and Watson, for example, derived a value for k_1 from a mass spectral analysis of OClO, ClO, and BrO temporal profiles resulting from reaction of OClO with excess Br. Toohey et al., on the other hand, measured k_1 directly by LMR detection of ClO decay in the presence of excess BrO.

The room-temperature value of k_1 obtained by Hills et al.,⁹ using mass spectrometric detection of BrO in the presence of excess ClO, is nearly 40% lower than the value obtained in the present work. The results reported by Hills et al. also suggest that k_1 is temperature independent. Consequently, the discrepancy between the two investigations increases with decreasing temperatures. At 220 K, for instance, the value measured for k_1 in this work is a factor of 2.6 larger than the value reported by Hills et al. The primary difference between the two studies is the use by Hills et al. of ClO and BrO sources employing O₃. Since the presence

(25) Clyne, M. A. A.; Coxon, J. A. *Proc. R. Soc. London, A* **1968**, *303*, 207.

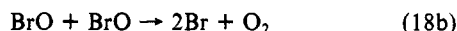
(26) Clyne, M. A. A.; Cruse, H. W. *Trans. Faraday Soc.* **1970**, *66*, 2214.

of O₃ leads to the secondary regeneration of BrO if Br is formed, caution must be exercised in the use of these sources. Hills et al. attempted to minimize this interference by maintaining O₃ concentrations below 2×10^{12} molecules cm⁻³ in the reaction zone. However, the extent to which reaction 3 interferes with measurements of BrO decay also depends on the Br concentration, i.e.

$$-d[\text{BrO}]/dt = k_1[\text{BrO}][\text{ClO}] - k_3[\text{Br}][\text{O}_3] \quad (\text{VI})$$

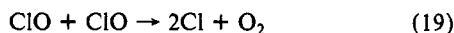
We believe that bromine atoms, which could not be measured directly by Hills et al., were present in sufficient quantities to significantly impact their rate coefficient determinations. As we will demonstrate, the origin of these relatively large Br concentrations is likely traced to the reaction of Br₂ with Cl (reaction 9).

The extent to which secondary chemistry was involved in the experiment of Hills et al. critically depended on the concentrations of Cl, Br, Br₂, and O₃. Concentration measurements were reported only for O₃, however. Hills et al. offered estimates of the Br and Cl concentrations ($[\text{Br}] \approx 4 \times 10^{11}$ and $[\text{Cl}] \approx 5 \times 10^{12}$ in units of atoms cm⁻³) but did not discuss the methods used to obtain these estimates. According to details given by Hills,²⁷ the estimate of $[\text{Br}]$ reported by Hills et al. was based on a model of BrO source chemistry. Br concentrations calculated from the model were of the same magnitude as the initial BrO concentrations owing to the occurrence of reaction 18b and the imposed limit of 2×10^{12} molecules cm⁻³ on $[\text{O}_3]$. The estimate of $[\text{Br}]$ did not include contributions from reactions 1a, 1b, or 9.



$$k_{18b} = 1.4 \times 10^{-12} \exp(150/T) \text{ cm}^3 \text{ molecule}^{-1} \text{ s}^{-1}$$

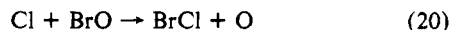
The basis for the reported estimate of $[\text{Cl}]$ is not delineated by either Hills et al.⁹ or Hills.²⁷ In fact, Hills concluded from a model of ClO source chemistry that Cl concentrations were on the order of 5×10^{10} atoms cm⁻³ rather than 5×10^{12} atoms cm⁻³ as claimed by Hills et al. In order to identify the origins and quantify the magnitudes of the sources of chlorine atoms in the Hills et al. experiment, we have simulated the chemistry occurring in their system. On the basis of experimental conditions given by Hills, we find, contrary to the conclusion reached by Hills, that the ClO source region is the major contributor of Cl to the reactor. According to our calculations, this source is responsible for Cl concentrations between 3×10^{12} and 7×10^{12} atoms cm⁻³ inside the reaction zone, a result that is in good agreement with the estimate reported by Hills et al. The low value of $[\text{Cl}]$ calculated by Hills results from neglect of ClO disproportionation inside the source region



$$k_{19}(298 \text{ K}) \approx 5.4 \times 10^{-15} \text{ cm}^3 \text{ molecule}^{-1} \text{ s}^{-1}{}^{14}$$

The impact of reaction 19 on the chemical composition of the ClO source effluent cannot be overemphasized. On account of reaction 19, it is virtually impossible to design a ClO source based on reaction 6, which yields negligible amounts of both Cl and O₃.

The effect of Cl concentrations near 5×10^{12} atoms cm⁻³ on measurements of reaction 1 depends critically on the concentrations of Br₂ present. For small Br₂ concentrations ($< 10^{11}$ molecules cm⁻³), BrO destruction by Cl (reaction 10) will be significant and will result in larger apparent rate constants for reaction 1. It is important to note that Hills et al. neglected to consider reaction 10 as a possible source of interference. Their assessment of the impact of chlorine atoms on BrO was confined to the reaction



which is slow on account of being approximately 4 kcal mol⁻¹ endothermic. For large Br₂ concentrations ($> 5 \times 10^{12}$ molecules cm⁻³), titration of Cl to Br by reaction 9 will be rapid. The presence of Br at levels 10 times greater than estimated by Hills

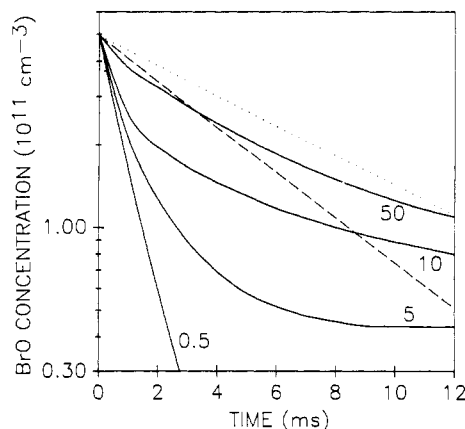


Figure 8. Simulation of the effects of reactions 3 and 10 on BrO decay observed by Hills et al.⁹ The solid lines are kinetics simulations for different Br₂ concentrations. Numbers shown are Br₂ concentrations in units of 10^{12} molecules cm⁻³. The experimental conditions used for the simulations are $T = 305 \text{ K}$; $k_1 = 1.30 \times 10^{-11} \text{ cm}^3 \text{ molecule}^{-1} \text{ s}^{-1}$; $[\text{ClO}] = 1.5 \times 10^{13}$ molecules cm⁻³, $[\text{BrO}]_0 = 5 \times 10^{11}$ molecules cm⁻³, $[\text{O}_3] = 2 \times 10^{12}$ molecules cm⁻³, and $[\text{Br}] = 5 \times 10^{12}$ molecules cm⁻³. The dashed and dotted lines are BrO decays (secondary chemistry omitted) calculated for k_1 values of 1.3×10^{-11} and $8.4 \times 10^{-12} \text{ cm}^3 \text{ molecule}^{-1} \text{ s}^{-1}$, respectively.

et al. will result in significant regeneration of BrO and will lead to smaller apparent rate coefficients for reaction 1.

Since Hills et al. do not report initial Br₂ concentrations for their kinetics experiments, we have modeled the BrO + ClO system for a range of Br₂ concentrations. The results of this analysis are shown in Figure 8 for a set of experimental conditions typical of the Hills et al. experiment, i.e., $T = 305 \text{ K}$, $[\text{ClO}]_0 = 1.5 \times 10^{13}$, $[\text{BrO}]_0 = 5 \times 10^{11}$, $[\text{O}_3]_0 = 2 \times 10^{12}$, $[\text{Br}]_0 = 4 \times 10^{11}$, and $[\text{Cl}]_0 = 5 \times 10^{12}$ (molecules (atoms) cm⁻³). For this calculation, k_1 was taken from the present work to be $1.3 \times 10^{-11} \text{ cm}^3 \text{ molecule}^{-1} \text{ s}^{-1}$.

The main conclusion of this analysis is that secondary chemistry affects observed BrO decays for all values of $[\text{Br}_2]$. Derived values of k_1 are equal to the actual value only at particular Br₂ concentrations and reaction time intervals, fortuitous occurrences resulting when BrO destruction by reaction 10 is approximately balanced by BrO regeneration from reaction 9. As can be evidenced from Figure 8, Br₂ concentrations greater than 5×10^{12} molecules cm⁻³ result in BrO loss rates, over most of the experimental time frame, that are similar to those measured by Hills et al. On the basis of this evidence, we conclude that the experiments of Hills et al. employed relatively high concentrations of Br₂. This conclusion is consistent with our experience concerning the efficiency of Br₂ dissociation in a microwave cavity under the experimental flow conditions employed by Hills et al. We also speculate that the failure of Hills et al. to detect curvature in their data may be attributable to two factors: the lack of temporal resolution for times less than 2 ms due to injector mixing effects and poor signal to noise ratios for BrO at longer reaction times.

We turn now to a comparison of product yields. OClO yields ranging between 45% and 55% have been reported by Clyne and Watson,⁸ Hills et al.,⁹ and Toohy et al.¹⁷ Considering the experimental difficulties inherent in studies of multichannel radical-radical reactions, these values must be considered in excellent agreement with one another as well as with the result of the present work. The product yields reported by Hills et al., although obtained in a system complicated by BrO regeneration, can be considered to be reliable since they were based on correlated changes in ClO and OClO. Neither of these species was adversely affected by the occurrence of reaction 3.

BrCl yield (reaction 1c) measurements have previously been attempted only by Hills et al.⁹ Their failure to detect BrCl production in the presence of isobutane, which served to scavenge Cl atoms and prevent reaction 9, led them to place an upper limit of 0.02 on the branching ratio for this channel. However, in view

(27) Hills, A. J. Ph.D. Thesis, University of Colorado, 1987.

of their stated BrCl sensitivity ($\approx 1.2 \times 10^{11}$ molecules cm^{-3} for $S/N = 2$) and maximum allowed BrO concentration (5×10^{11} molecules cm^{-3}), it is difficult to justify such a low limit. Moreover, the electron capture cross section for isobutane is sufficiently large as to degrade the sensitivity of the mass spectrometer when excess isobutane is employed. Accordingly, an upper limit greater than 0.12 for the BrCl branching ratio appears to be more consistent with the reported data. This latter upper limit is consistent with the values obtained in the present work.

Qualitative evidence in support of a significant yield of BrCl in reaction 1 can be inferred from previously reported observations of BrCl($^3\pi_0^+$) emission from reaction mixtures of Br and OClO.²⁸⁻³⁰ Although initially this emission was attributed to the reaction of Br with ClOO,³⁰ this conclusion was based on an incorrectly low estimate of the ClOO decomposition rate. Alternatively, the occurrence of reaction 1c, where the nascent BrCl is electronically excited, provides a straightforward explanation for these observations. Recently, Toohey et al.¹⁷ have shown that a model containing reaction 1c can predict the previously observed BrCl emission. They have also presented data on the yields of bromine atoms from reaction 1 that suggest a significant role for reaction 1c.

Implications for Atmospheric Chemistry. Following the revelation by Farman et al.¹⁰ of an unprecedented drop in the

springtime levels of ozone over the Antarctic region, a host of theories were proposed to explain this phenomenon. McElroy et al.¹¹ first emphasized the possible role of reaction 1a in the destruction of O₃ under the special conditions existing in Antarctica. Ground-based observations of OClO made by Solomon et al.³¹ at McMurdo Station have provided solid albeit circumstantial evidence for the occurrence of reaction 1. Recent attempts to model the role of reaction 1 in the Antarctic stratosphere have employed the room-temperature rate coefficient data of Clyne and Watson.^{11,32} The present results reveal that the rate coefficient for reaction 1 depends inversely on temperature. Consequently, for temperatures typical of the Antarctic stratosphere (190 K), reaction 1 will take on added significance. In addition, the identification of reaction 1c, previously omitted in model calculations, provides a means for sequestering BrO during the night. The significance of these new findings is discussed in ref 33.

Acknowledgment. We thank Drs. D. W. Toohey and R. J. Salawitch for many helpful discussions. The research described in this paper was carried out at the Jet Propulsion Laboratory, California Institute of Technology, under contract to the National Aeronautics and Space Administration.

Registry No. ClO, 14989-30-1; BrO, 15656-19-6.

(28) Clyne, M. A. A.; Coxon, J. A. *Proc. R. Soc. London, A* **1967**, *298*, 424.

(29) Hadley, S. G.; Bina, M. J.; Brabson, G. D. *J. Phys. Chem.* **1974**, *78*, 1833.

(30) Clyne, M. A. A.; Toby, S. J. *J. Photochem.* **1979**, *11*, 87.

(31) Solomon, S.; Mount, G. H.; Sanders, R. W.; Schmeltekopf, A. L. *J. Geophys. Res., D: Atmos.* **1987**, *92*, 8329.

(32) Rodriguez, J. M.; Ko, M. K. W.; Sze, N. D. *Geophys. Res. Lett.* **1986**, *13*, 1292.

(33) Sander, S. P.; Friedl, R. R. *Geophys. Res. Lett.* **1988**, *15*, 887.

Kinetics and Product Studies of the Reaction ClO + BrO Using Flash Photolysis-Ultraviolet Absorption

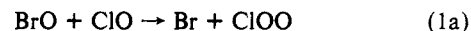
Stanley P. Sander* and Randall R. Friedl

Jet Propulsion Laboratory, California Institute of Technology, Pasadena, California 91109
(Received: August 10, 1988; In Final Form: December 20, 1988)

The flash photolysis-ultraviolet absorption method has been used to study the BrO + ClO reaction over the pressure range 50–700 Torr and temperature range 220–400 K. The rate constant for the overall reaction is given by $k_1 = (6.1 \pm 1.2) \times 10^{-12} \exp[(240 \pm 60)/T] \text{ cm}^3 \text{ molecule}^{-1} \text{ s}^{-1}$ ($\pm 2\sigma$ error limits). Branching ratios for the reaction channel forming OClO were determined at 220 and 298 K and found to be 0.68 ± 0.10 and 0.59 ± 0.10 , respectively. Absolute UV absorption cross sections for ClO and BrO were determined as a function of temperature at the peaks of the 12–0 and 7–0 bands. In order to more fully understand the reaction mechanism used in the BrO + ClO study, the reactions $\text{Br} + \text{Cl}_2\text{O} \rightarrow \text{ClO} + \text{BrCl}$ and $\text{Cl}_2\text{O} + h\nu \rightarrow \text{products}$ were examined. The Arrhenius expression for the $\text{Br} + \text{Cl}_2\text{O}$ reaction was found to be $k_3 = (2.1 \pm 1.8) \times 10^{-11} \exp[-(520 \pm 260)/T] \text{ cm}^3 \text{ molecule}^{-1} \text{ s}^{-1}$ ($\pm 2\sigma$) over the temperature range 220–298 K. The quantum yield for the production of atomic oxygen from broad-band Cl₂O photolysis ($\lambda > 180 \text{ nm}$) was found to be 0.25 ± 0.05 .

Introduction

The BrO + ClO reaction is an important process in the chemistry of the Earth's stratosphere because it links the catalytic ozone destruction cycles of the chlorine and bromine radical families. While the role that this reaction plays in the chemistry of the midlatitude stratosphere has been understood for some time,¹ the recent discovery of a massive springtime decline in the stratospheric ozone column over Antarctica has stimulated renewed interest in this reaction.² Data needs have focused on the temperature and pressure dependences of the rate coefficients for the three exothermic product channels



The previous paper³ has discussed an experimental approach to this reaction that utilized the technique of discharge-flow mass spectrometry. In order to validate the results of that technique and to extend the pressure regime over the full 1–700-Torr range, we have studied reaction 1 using the flash photolysis-ultraviolet absorption method. Rate constants for reaction 1 were obtained over the temperature range 220–400 K and the branching ratio k_{1b}/k_1 was determined at 220 and 298 K by monitoring the

(1) Yung, Y. L.; Pinto, J. P.; Watson, R. T.; Sander, S. P. *J. Atmos. Sci.* **1980**, *37*, 339.

(2) McElroy, M. B.; Salawitch, R. J.; Wofsy, S. C.; Logan, J. A. *Nature* **1986**, *321*, 759.

(3) Friedl, R. R.; Sander, S. P. *J. Phys. Chem.*, preceding paper in this issue.